Relationships between Atomic Diffusion Mechanisms and Ensemble Transport Coefficients in Crystalline Polymorphs

Benjamin J. Morgan*
Department of Materials, University of Oxford, Parks Road, Oxford OX1 3PH, United Kingdom and Stephenson Institute for Renewable Energy, Department of Chemistry, University of Liverpool, Liverpool L69 3BX, United Kingdom

Paul A. Madden
Department of Materials, University of Oxford, Parks Road, Oxford OX1 3PH, United Kingdom
(Received 24 July 2013; published 8 April 2014)

Ionic transport in conventional ionic solids is generally considered to proceed via independent diffusion events or "hops." This assumption leads to well-known Arrhenius expressions for transport coefficients, and is equivalent to assuming diffusion is a Poisson process. Using molecular dynamics simulations of the low-temperature $B1$, $B3$, and $B4$ AgI polymorphs, we have compared rates of ion hopping with corresponding Poisson distributions to test the assumption of independent hopping in these common structure types. In all cases diffusion is a non-Poisson process, and hopping is strongly correlated in time. In $B1$ the diffusion coefficient can be approximated by an Arrhenius expression, though the physical significance of the parameters differs from that commonly assumed. In low temperature $B3$ and $B4$, diffusion is characterized by concerted motion of multiple ions in short closed loops. Diffusion coefficients cannot be expressed in a simple Arrhenius form dependent on single-ion free energies, and intrinsic diffusion must be considered a many-body process.

DOI: 10.1103/PhysRevLett.112.145901 PACS numbers: 66.30.-h, 41.20.Cv, 66.30.Dn, 66.30.Lw

Ionic transport in crystalline solids is a fundamental process of prime importance to solid-state reactions and the behavior of solid-state devices such as batteries, fuel cells, and chemical sensors. Mass and charge transport are characterized by diffusion coefficients and ionic conductivities, respectively. Differences in transport rates between materials depend on the relationships between these ensemble transport coefficients and the microscopic diffusion mechanisms that govern the motion of individual ions. A long-standing question in this regard is how this relationship between microscopic and macroscopic descriptions of transport varies with crystal structure [1]. Here we focus on "conventional" ionic structures, such as wurtzite and rocksalt, that are intrinsically poor ionic conductors. Understanding the relationship between structure and transport in these materials is motivated in part by observations of greatly enhanced conductivities when they are prepared in nanoscale particles [2,3], where local structure effects may be significant.

The strong effect of crystal structure on ionic transport is exemplified by the ionic conductivities of AgI polymorphs. Under ambient conditions AgI forms the thermodynamically preferred wurtzite-structured ($B4$) β phase or the metastable zinc-blende-structured ($B3$) γ phase. Both phases are poor ionic conductors: at 420 K the conductivity of β AgI is $\sim 4.5 \times 10^{-4}\ \Omega^{-1}\,\mathrm{cm}^{-1}$ [4], and molecular dynamics simulations predict an even lower intrinsic ionic conductivity for γ AgI [5]. Above 420 K β AgI undergoes a phase transition to the superionic α phase, in which the iodide ions are arranged in a bcc lattice with the mobile silver ions distributed over one sixth of the available tetrahedral sites [6,7]. The $\beta \rightarrow \alpha$ transition is associated with an increase in silver-ion conductivity of over 3 orders of magnitude [8]. Applying pressure to β AgI causes a phase transition to a rocksalt-structured ($B1$) phase above 1.0 GPa, associated with an increase in room-temperature conductivity of 2 orders of magnitude [9].

The excellent silver ion mobility of α AgI is attributed to the high concentration of vacant sites in the silver sublattice, which gives low activation barriers to diffusion [6,7]. In contrast, the low-temperature $B1$, $B3$, and $B4$ phases have fully occupied silver sublattices in the perfect crystals, and ionic transport is expected to occur via conventional Frenkel pair "hopping" mechanisms, where thermally generated vacancies and interstitials diffuse by a series of discrete events or hops [10].

For a generic hopping diffusion mechanism, if ion hopping occurs at random (i.e., hopping probabilities of individual ions are statistically independent) then application of Vineyard's absolute rate theory allows the diffusion coefficient D to be written in the well-known Arrhenius form [11,12]:

$$D \propto n \exp\left(-\Delta G_{\mathrm{hop}}/kT\right), \tag{1}$$

where n is the number of species capable of effecting hops per unit volume, and ΔG_{hop} is the free energy barrier associated with the motion of a single ion [10,11]. In an ionic crystal n is usually considered to be the concentration of point defects:

$n = n_{\mathrm{def}}$. At low temperatures n_{def} is fixed by the concentration of extrinsic aliovalent dopants or impurities and is independent of temperature. At high temperatures intrinsic defect formation can dominate n_{def} and the expression for D can be modified to take this into account: e.g., for a Frenkel disordered material, such as the low-temperature phases of AgI, $n_{\mathrm{def}} = \exp(-\Delta G_{\mathrm{FP}}/2kT)$, with ΔG_{FP} the free energy for Frenkel pair formation. This independent hopping model predicts an Arrhenius plot of $\log(D)$ versus $1/T$ will consist of a series of straight lines. The slope of each line defines an activation energy that is linearly dependent on free energy differences conceptually associated with displacements of individual ions. Because this derivation relies on the application of absolute rate theory, it is important for the understanding of ionic transport in conventional (non-superionic) ionic solids to be able to test the assumption of independently occurring hops.

If ionic hopping is a random process the probability of a specific hop occurring in time Δt depends only on the average hopping rate. This is formally equivalent to requiring that ion hopping is a Poisson process with a frequency distribution of

$$P_k(\lambda) = \frac{\lambda^k e^{-\lambda}}{k!}, \tag{2}$$

where P_k is the probability of observing k events in time window Δt, and λ is the mean number of events in all equivalent time windows [13].

In this Letter we describe molecular dynamics simulations of the $B1$, $B3$, and $B4$ polymorphs of AgI. By expressing diffusion as a series of discrete diffusion events (hops) we directly compare hopping frequency probabilities against equivalent Poisson distributions to test the validity of the independent hopping model. In the $B1$, $B3$, and $B4$ low-temperature phases of AgI we find intrinsic diffusion is a non-Poisson process and ion hops are strongly correlated in time. The dominant transport mechanism varies with lattice structure, which manifests as qualitatively different relationships between ensemble diffusion coefficients and ionic conductivities for the tetrahedrally coordinated $B3$ and $B4$ phases versus the octahedrally coordinated $B1$ phase.

Constant volume molecular dynamics simulations were performed using the PRV rigid-ion potential [14], with a time step of 200 au (4.84 fs), for a total length of 3.2×10^6 steps (~15.5 ns) at each temperature. System sizes were $B4$: 896 ions, B3: 1008 ions, $B1$: 1000 ions. The $B4$ and $B3$ calculations used an optimized zero-pressure volume obtained for stoichiometric $B4$ AgI at 0 K of 71.68 Å^3 per molecular unit and a c/a ratio of 1.6, following the procedure of Zimmer *et al.* [15]. The high-pressure $B1$ phase was simulated at a volume of 67.27 Å^3 per molecular unit, which gives sufficient positive pressure to stabilize this high-pressure phase across the range of simulation temperatures [16].

Ionic conductivities σ, and Ag^+ diffusion coefficients $D(Ag^+)$ were calculated from the long-time slopes of the charge density and individual ion position mean-squared displacements, respectively [5]. The ionic conductivities are ordered $B3 < B4 \ll B1$ [Fig. 1(a)], which is consistent with the experimentally observed $\times 10^2$ conductivity increase at room temperature for $B1$ AgI relative to $B4$ [9]. The Ag^+ diffusion coefficients show the same trend as the ionic conductivities [Fig. 1(b)]. Statistical errors for the diffusion coefficients are reduced compared with the conductivities because of the additional averaging over Ag^+ ions, and the diffusion data plotted as $\log(D)$ versus $1000/T$ appear as straight lines, suggesting Arrhenius-like behavior.

σ and D are related by the Nernst-Einstein equation,

$$\frac{\sigma}{D} = \frac{nq^2}{kT} f_{\mathrm{NE}}, \tag{3}$$

where n is the number of mobile ions per unit volume and q their charge. f_{NE} is the Nernst-Einstein factor. In cases where ionic motion is correlated, charge and mass transport are not equivalent and f_{NE} deviates from unity. For independent vacancy and interstitial hopping mechanisms

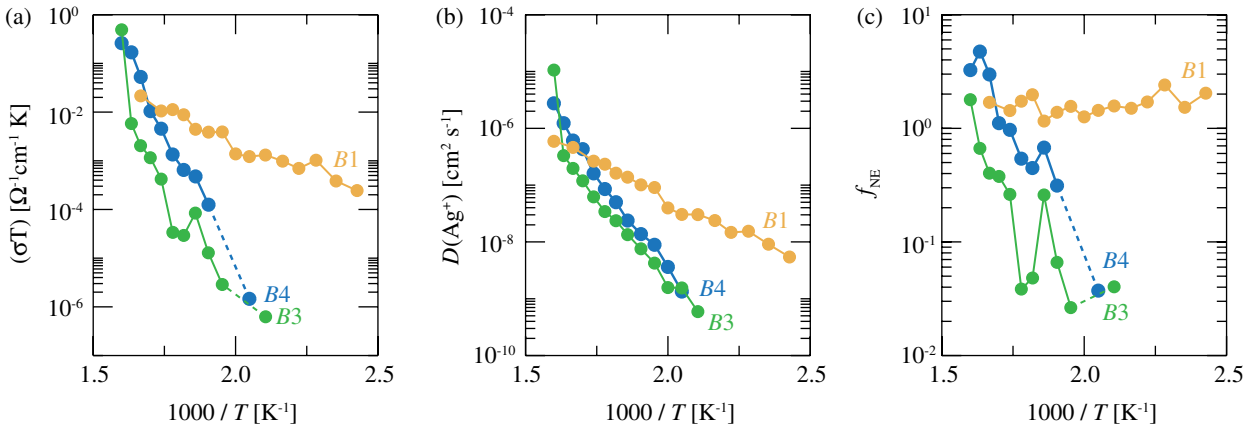

FIG. 1 (color online). Calculated transport coefficients for $B1$, $B3$, and $B4$ AgI: (a) Ionic conductivities, σ; (b) Ag^+ diffusion coefficients, $D(Ag^+)$; (c) Nernst-Einstein factor, f_{NE}. Dashed lines in (a) indicate conductivities too small to measure, giving $f_{\mathrm{NE}} \to 0$ in these regions in (c).

in the $B1$, $B3$, and $B4$ lattices calculated values of f_{NE} are in the range 1–3 [17]. Values of f_{NE} from the simulation data are shown in Fig. 1(c). For $B1$ $f_{\mathrm{NE}} \approx 1.4$ across the temperature range, which is consistent with a combination of independent vacancy and interstitial hopping by thermally generated Frenkel pairs. $B3$ and $B4$, however, show a strong temperature dependence: $f^{\mathrm{NE}} \approx 1$ at high temperatures but decays approximately exponentially as the temperature decreases. The low temperature values of $f_{\mathrm{NE}} \ll 1$ are inconsistent with the calculated values for independent vacancy or interstitial hopping [17], which suggests that alternate diffusion mechanisms mediate intrinsic Ag^+ transport in $B3$ and $B4$ AgI.

For the independent hopping model to be valid it is necessary that ion hopping is a Poisson process. For each simulation trajectory we have expressed the ionic transport process as sequences of "diffusion events." At every time step each Ag^+ ion occupies a specific lattice or interstitial site [18]. If a Ag^+ ion moves out of a lattice site, it must later either return to this same site, in which case the sequence does not contribute to diffusion and is discarded, or occupy a second lattice site. The process of a Ag^+ ion moving from one lattice site to another is classified as a diffusion event or hop. Any such process occurs over a number of simulation steps, and to simplify our analysis we define a diffusion event as being coincident with the final site occupation. The set of diffusion events provides a discretized microscopic description of the diffusion dynamics throughout a simulation. In the AgI systems modeled here, nearly all diffusion events consist of motion between nearest-neighbor lattice sites, and the average rate of these hops is proportional to the macroscopic diffusion coefficient (cf. Supplemental Material, Fig. S1 [19]) [20].

For any discrete process, the probability of k events occurring in time Δt is described by the probability mass function (PMF). Figures 2(a) and 2(b) show diffusion event PMFs observed for *nonstoichiometric* $B1$, $B3$, and $B4$ AgI simulations, constructed with two Ag^+ ions either removed or added to give an excess of vacancies or interstitials. Under these conditions diffusion is dominated by the hopping of these *extrinsic* point defects. Comparing these PMFs with exact Poisson distributions for the same average values of k shows close agreement: under nonstoichiometric conditions transport of excess Ag^+ vacancies and interstitials is consistent with independent hopping and the derivation that leads to Eq. (1) is valid. For stoichiometric $B1$, $B3$, and $B4$, however, there are large discrepancies between the diffusion event PMFs and the corresponding Poisson distributions (the "goodness of fit" between calculated PMFs and corresponding exact Poisson distributions [21,22] is quantified in the Supplemental Material [19]). All three polymorphs show non-Poisson diffusion, even though f_{NE} deviated from values for independent hopping processes only for the $B3$ and $B4$ phases.

The disagreement between the diffusion event PMFs and the corresponding exact Poisson distributions indicates

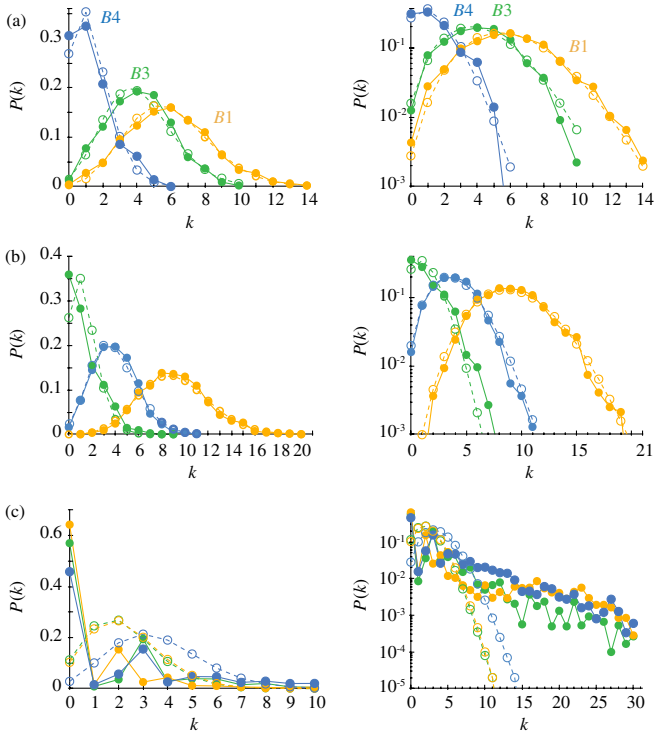

FIG. 2 (color online). PMFs for k diffusion events observed in time $\Delta t = 12\,500$ time steps (≈60.5 ps). Simulation data (filled circles) are shown for $B1$ (yellow), $B3$ (green), and $B4$ (blue) AgI on both linear (left panels) and $\log_{10}$ (right panels) scales. (a) Excess vacancies (300 K/350 K/350 K) (b) Excess interstitials (300 K/350 K/350 K) (c) Stoichiometric (450 K/550 K/550 K). Open circles (dashed lines) show exact Poisson distributions with equivalent values of $\langle k \rangle$. Data for stoichiometric $B4$ (550 K) with $\Delta t = 2500$ to 62 500 time steps are included in the Supplemental Material (Fig. S3) [19].

temporal correlation between intrinsic diffusion events in $B1$, $B3$, and $B4$ AgI. This is also evident in running totals of diffusion events taken from individual representative simulations (Fig. 3). Within any single analysis frame (250 time steps ≈ 1.2 ps) no single diffusion events are observed. Diffusion events occur in clusters that are separated by long times containing zero diffusion events. The $B1$ data exhibit "cascades" of multiple diffusion events (Fig. 3) as well as smaller clusters containing only a few events.

The non-Poisson hopping statistics for these low temperature phases mean that intrinsic ionic transport in these materials cannot be described as a simple average over independent diffusion events. Instead, examining the relationships between individual diffusion events is necessary to understand the net contributions to mass and charge transport. The relationship between individual diffusion events can be described by constructing "diffusion chains." These chains are constructed by connecting pairs of events that share one common lattice site as the origin site for one event and the destination site for the second event. A diffusion event cannot be completed before the ion originally

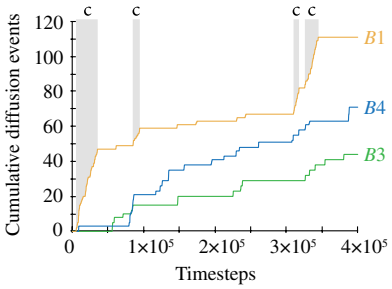

FIG. 3 (color online). Cumulative diffusion events from sample molecular dynamics trajectories. $B1$: 450 K, $B3$, and $B4$: 550 K. The regions shaded grey and marked c are examples of "cascades" discussed in the text, and used for the analysis presented in Fig. 4.

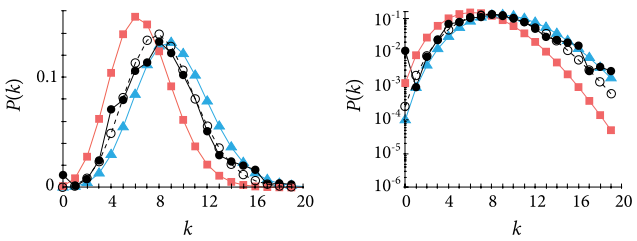

FIG. 4 (color online). PMF for k diffusion events for stoichiometric $B1$ at 450 K in time $\Delta t = 5000$ time steps, only considering sections of trajectories where cascades of diffusion events are observed (solid black circles). The corresponding exact Poisson distribution is shown in open black circles. PMFs for extrinsic vacancy and interstitial diffusion in $B1$ AgI at the same temperature are shown in red squares and blue triangles, respectively.

occupying the destination site departs, thus initiating a second diffusion event that can, in turn, only be completed after a third accessible site is vacated (see Supplemental Material [19], Fig. S2) [23]. This definition of chains provides a course-grained description of transport that ignores the chronological order of diffusion events. The net contribution of a chain to $D(\mathrm{Ag}^+)$ is proportional to the number of diffusion events in each chain, whereas the contribution to σ depends on the vector sum of all component diffusion events.

In a stoichiometric system, diffusion chains are initiated by Frenkel pair formation and terminated by Frenkel pair recombination. To understand the contribution specific chains make towards ensemble diffusion and conductivity it is instructive to consider the limits of "long" versus "short" chains. For long chains the transport behavior will approximate that of a well-separated noninteracting vacancy and interstitial pair, with each defect expected to diffuse by an independent hopping process that obeys Poisson statistics. This "open chain" behavior is exhibited during the multiple-hop cascades observed in the $B1$ simulations (cf. Fig. 3). The diffusion event PMF generated by analyzing only these cascades closely follows the corresponding exact Poisson distribution, and is quantitatively consistent with an average of the hopping rates from nonstoichiometric excess vacancy and interstitial simulations performed at the same temperature. Because transport in long chains tends to that of independent vacancy-interstitial pairs, in a system where long chains dominate transport f_{NE} is predicted to be ≈ 1. The limit of short chains corresponds to closed loops. Although the contribution to ensemble diffusion is the same as in the open-chain limit, proportional to the number of diffusion events in the chain, the contribution to the ionic conductivity is zero, because a closed loop of diffusion events gives no net displacement of charge. For a system where transport is effected predominantly by short chains this predicts $f_{\mathrm{NE}} \to 0$.

The relationship between chain length and contribution to ionic conductivity in these limiting cases suggests that the contrasting behavior of f_{NE} in $B1$, $B3$, and $B4$ is connected to the distribution of chain lengths for each simulation. As a coarse measure of whether diffusion occurs predominantly in short versus long chains, we calculate the probability that a diffusion event in a simulation occurs in a chain of length < 5, denoted $P_{\{3,4\}}$ [Fig. 5(a)] [24]. The relative contribution to transport from short versus long chains can then be expressed as a free energy difference $\Delta G_{\{3,4\}}$;

$$\Delta G_{\{3,4\}} = -kT \ln \frac{P_{\{3,4\}}}{1 - P_{\{3,4\}}}, \tag{4}$$

plotted in Fig. 5(b). For $B1$, $P_{\{3,4\}}$ is low at all temperatures ($\Delta G_{\{3,4\}} > 0$). Ionic transport is dominated by diffusion events in extended chains, and behaves approximately as for independent vacancy-interstitial pairs. Neglecting contributions from the small proportion of short chains, $D(\mathrm{Ag}^+)$ can be expressed in an Arrhenius form that depends on the free energy associated with forming *independent* vacancy-interstitial Frenkel pairs, ΔG_{iFP}:

$$D \propto \exp\left(-\Delta G_{\mathrm{iFP}}/2kT\right) \exp\left(-\Delta G_{\mathrm{hop}}/kT\right). \tag{5}$$

For $B3$ and $B4$ at low temperatures $P_{\{3,4\}}$ is high ($\Delta G_{\{3,4\}} < 0$). Transport is characterized by short chains, which must be closed loops and therefore do not contribute to ionic conductivity. This explains the strong deviations from Nernst-Einstein behavior at low temperatures in these phases. With increasing temperature a greater proportion of

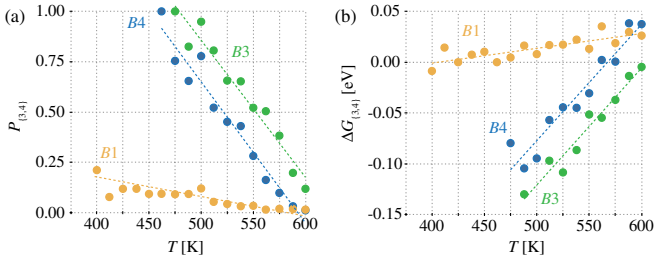

FIG. 5 (color online). (a) Probability of a diffusion event occurring within a chain of length 3 or 4 (b) Free energy difference between a diffusion event occurring in a chain of length 3 or 4 versus a longer chain [Eq. (4)]. Key: $B1$ (yellow), $B3$ (green), and $B4$ (blue).

diffusion events occur within extended chains ($\Delta G_{\{3,4\}}$ approaches 0). This is consistent with the increase of f_{NE} with temperature, and the recovery of "normal" Nernst-Einstein behavior at high T. The coincident increase of $D(\mathrm{Ag}^+)$ and f_{NE} with temperature predicts a rapid increase of σ with T. This is consistent with experimental super-Arrhenius conductivities observed for $B3$ and $B4$ AgI, and suggests this phenomenon can be explained by a switch in the dominant transport mechanism from short to long chains with increasing temperature [4,25].

We have shown that the common assumption that ionic transport occurs by independent hops of mobile ions is invalid for stoichiometric $B1$, $B3$, and $B4$ AgI, which can be considered representative of conventional (nonsuperionic) crystalline solids. For diffusion in the stoichiometric materials, thermally created Frenkel pairs do not necessarily dissociate into independent vacancies and interstitials. This has consequences for the relationship between the hopping statistics of individual ions and the ensemble transport coefficients measured in experiments. We have identified two classes of non-Poisson ion hopping, which are distinguished by the spatial correlations between hops. When diffusion occurs via extended open chains of hops then defects behave similarly to noninteracting species, and the diffusion coefficient can be expressed in an approximate Arrhenius form [Eq. (5)]. Alternately, when diffusion occurs via short closed loops of hops then diffusion coefficients cannot be expressed in a simple Arrhenius form that depends only on single-ion free energies, and intrinsic diffusion must be considered a many-body process. In general, intrinsic diffusion in $B1$, $B3$, and $B4$-structured materials should not be assumed to occur via independent hopping, and it may not be possible to relate activation energies for experimental transport coefficients to microscopic free energy barriers involving the motion of single ions [26]. Although we are not aware of experimental data that confirm these findings, we hope that the demonstration that ionic transport in even structurally simple ionic solids can be much more complex than previously assumed will stimulate experimental studies in this area.

For AgI the octahedrally coordinated $B1$ phase exhibits predominantly open chain diffusion, whereas the tetrahedrally coordinated $B3$ and $B4$ phases at low temperatures exhibit predominantly closed chain diffusion, showing defect pairs remain much more strongly bound in the tetrahedral $B3$ and $B4$ phases than the $B1$ phase. This qualitative difference in mechanism is consistent with the increase in conductivity of 2 orders of magnitude during the pressure-driven $B4 \rightarrow B1$ phase transition in AgI. Including the superionic α phase, AgI therefore exhibits a remarkable variation between three qualitatively different transport mechanisms within the same material, purely as a function of crystal structure.

This work was supported by EPSRC Grant No. EP/H003819/1.

*bmorgan@liv.ac.uk

[1] L. V. Azároff, J. Appl Phys. **32**, 1658 (1961).
[2] J. Maier, Phys. Chem. Chem. Phys. **11**, 3011 (2009).
[3] E. M. Chan, M. A. Marcus, S. Fakra, M. ElNaggar, R. A. Mathies, and A. P. Alivisatos, J. Phys. Chem. A **111**, 12 210 (2007).
[4] R. J. Cava and E. A. Rietman, Phys. Rev. B **30**, 6896 (1984).
[5] B. J. Morgan and P. A. Madden, J. Phys. Condens. Matter **24**, 275303 (2012).
[6] P. A. Madden, K. F. O'Sullivan, and G. Chiarotti, Phys. Rev. B **45**, 10 206 (1992).
[7] S. Hull, Rep. Prog. Phys. **67**, 1233 (2004).
[8] C. Tubandt and E. Lorentz, Z. Phys. Chem. **87**, 513 (1914).
[9] A. Hao, C. Gao, M. Li, C. He, X. Huang, G. Zou, Y. Tian, and Y. Ma, J. Appl. Phys. **101**, 053701 (2007).
[10] The necessary conditions for ionic motion to be described in terms of discrete hops are discussed in C. R. A. Catlow, Solid State Ionics **8**, 89 (1983). Although diffusion in α-AgI can also be described as hopping between tetrahedral sites, the timescales of site residence and jump processes are of the same order of magnitude and the assumption used in simple hopping models that the residence time is much greater than the jump time is not valid.
[11] C. R. A. Catlow, Annu. Rev. Mater. Sci. **16**, 517 (1986).
[12] G. H. Vineyard, J. Phys. Chem. Solids **3**, 121 (1957).
[13] F. A. Haight, *Handbook of the Poisson Distribution* (Wiley, New York, 1967).
[14] M. Parrinello, A. Rahman, and P. Vashishta, Phys. Rev. Lett. **50**, 1073 (1983).
[15] F. Zimmer, P. Ballone, J. Maier, and M. Parrinello, J. Chem. Phys. **112**, 6416 (2000).
[16] Simulation cell volumes were 64 225 Å^3 for $B4$, 72 253 Å^3 for $B3$, and 67 270 Å^3 for the high-pressure $B1$ phase.
[17] K. Compaan and Y. Haven, Trans. Faraday Soc. **52**, 786 (1956); **54**, 1498 (1958).
[18] The procedure for assigning ions to lattice sites by geometric construction is described in Ref. [5].
[19] See Supplemental Material at http://link.aps.org/supplemental/10.1103/PhysRevLett.112.145901 for details.
[20] The observation that nearly all diffusion events occur between neighbouring lattice sites contradicts the proposal of Lee et al. that the dominant low-temperature diffusion mechanism in B4 AgI is pure interstitial diffusion along c-oriented channels of face-sharing octahedra: see J.-S. Lee, S. Adams, and J. Maier, J. Phys. Chem. Solids **61**, 1607 (2000).
[21] V. Choulakian, R. A. Lockhart, and M. A. Stephens, Can. J. Stat. **22**, 125 (1994).
[22] J. J. Spinelli and M. A. Stephens, Can. J. Stat. **25**, 257 (1997).
[23] The construction of chains of diffusion events is similar to the analysis of Wolf and Catlow used to identify "causal chains" of ion trajectories in Li_3N: M. L. Wolf and C. R. A. Catlow, J. Phys. C **17**, 6635 (1984).
[24] Chains of length 2 correspond to Frenkel pair formation and immediate recombination, with no contribution to either mass or charge transport, and are discounted from this analysis.
[25] J. R. Patnaik and C. S. Sunandana, J. Phys. Chem. Solids **59**, 1059 (1998).
[26] We expect nonstoichiometric systems will also exhibit non-Poisson diffusion processes, but that these make a negligible contribution towards ensemble transport except for cases of very limited nonstoichiometry.